EBioMedicine 60 (2020) 102986

Contents lists available at ScienceDirect

EBioMedicine

journal homepage: www.elsevier.com/locate/ebiom

Research paper

Autophagy induction promotes renal cyst growth in polycystic kidney disease

Eun Ji Lee[a,1], Je Yeong Ko[a,1], Sumin Oh[a], Jaehee Jun[a], Hyowon Mun[a], Chae Ji Lim[b], Seungwoon Seo[b], Hyuk Wan Ko[d], Hyunho Kim[e], Yun Kyu Oh[f], Curie Ahn[g], Minyong Kang[c], Min Jung Kim[a], Kyung Hyun Yoo[a], Goo Taeg Oh[b,*], Jong Hoon Park[a,*]

[a] Department of Biological Science, Sookmyung Women's University, Seoul 04310, Republic of Korea
[b] Department of Biology, Ewha Womans University, Seoul 03760, Republic of Korea
[c] Department of Urology, Samsung Medical Center, Sungkyunkwan University School of Medicine, Seoul 06351, Republic of Korea
[d] Department of Biochemistry, Yonsei University, Seoul 03722, Republic of Korea
[e] Center for Medical Innovation, Biomedical Research Institute, Seoul National University Hospital, Seoul 03082, Republic of Korea
[f] Department of Internal Medicine, Seoul National University Boramae Medical Center, Seoul 07061, Republic of Korea
[g] Department of Internal Medicine, Seoul National University College of Medicine, Seoul 03080, Republic of Korea

ARTICLE INFO

Article History:
Received 18 July 2020
Revised 14 August 2020
Accepted 19 August 2020
Available online xxx

Keywords:
Polycystic kidney
PKD
Autophagy
Ift46

ABSTRACT

Background: Polycystic kidney disease (PKD) involves renal cysts arising from proliferating tubular cells. Autophagy has been recently suggested as a potential therapeutic target in PKD, and mammalian target of rapamycin (mTOR) is a key negative regulator of autophagy. However, the effect of autophagy regulation on cystogenesis has not been elucidated in PKD mice.
Methods: Clinical validation was performed using GEO datasets and autosomal dominant polycystic kidney disease (ADPKD) patient samples. Newly established PKD and LC3 transgenic mice were used for *in vivo* verifications, and additional tests were performed *in vitro* and *in vivo* using multiple autophagy drugs.
Findings: Neither autophagy stimulation nor LC3 overexpression alleviated PKD. Furthermore, we observed the inhibitory effect of an autophagy inhibitor on cysts, indicating its possible therapeutic use in a specific group of patients with ADPKD.
Interpretation: Our findings provide a novel insight into the pathogenesis related to autophagy in PKD, suggesting that drugs related to autophagy regulation should be considered with caution for treating PKD.
Funding Sources: This work was supported by grants from the Bio & Medical Technology Development Program; the Collaborative Genome Program for Fostering New Post-Genome Industry of the NRF; the Basic Science Program.

1. Introduction

Polycystic kidney disease (PKD) is a highly prevalent genetic disease in which renal epithelia-lined cysts appear in both kidneys. Numerous fluid-filled cysts, the evident pathology of the disease, arise mainly from abnormally proliferating renal tubular cells, accompanied by inflammation, fibrosis, and finally lead to renal failure [1, 2]. Specifically, multiple molecular pathways, including cyclic AMP (cAMP) accumulation, enhanced vasopressin-specific signals, and hyper-activation of both mammalian target of rapamycin (mTOR) and mitogen activated protein (MAP) kinase signals are implicated in cyst growth [3-5]. Recently, autophagy has been suggested as another aberrant signaling pathway in PKD [6]. Autophagy is an intracellular process in which harmful or misfolded proteins are eliminated and normal energy levels are maintained. Upon cellular stresses such as nutrient starvation, damaged cytosolic proteins are enclosed by double-membrane vesicles called autophagosomes that fuse with lysosomes for degrading the cargo proteins. More than 30 autophagy-related genes (*ATGs*) are involved in this process and mTOR is one of the key negative regulators [7-9]. Since mTOR signal is generally enhanced in PKD, recent studies have attempted to identify the implication of autophagy in disease progression. Autophagy defects in numerous rodent models with polycystic kidneys as well as autophagy-stimulating effects of PKD drugs have been described in recent studies [6]. Moreover, identification of the therapeutic effect

* Corresponding author.
E-mail addresses: gootaeg@ewha.ac.kr (G.T. Oh), parkjh@sookmyung.ac.kr (J.H. Park).
[1] These authors contributed equally to this work.

https://doi.org/10.1016/j.ebiom.2020.102986

Research in Context section

Evidence before this study: Polycystic kidney disease (PKD) is a common genetic disease in which multiple renal cysts appear owing to germline mutations of ciliary proteins. The mTOR signal is generally enhanced in PKD, and multiple drugs targeting mTOR have been reported to reduce renal cystogenesis in PKD rodent models. In addition, mTOR is a key negative regulator of autophagy, therefore, autophagy has been increasingly suggested as another new therapeutic target of PKD. Recently, an autophagy activator has been shown to inhibit cysts in a zebrafish model; however, no further studies have been conducted using other vertebrate models.

Added value of this study: This study for the first time tries to link autophagy and PKD using vertebrate models. We have newly established *Ift46*-targeted PKD mice, and *LC3* overexpression unexpectedly increased cyst development, which worsened under autophagy stimulation. In addition, we observed the inhibitory effect of an autophagy inhibitor on cysts, indicating its possible therapeutic use in a specific group of PKD patients with altered autophagy.

Implications of all the available evidence: Compared to what the majority of researchers worldwide have observed in diverse rodent models, no significant clinical benefits of mTOR-targeting drugs have been reported. Our findings provide novel evidence to explain the limited therapeutic effects of mTOR inhibition in patients with PKD, wherein limited permissible doses in clinical trials as well as low tissue specificity were considered as the limitations until date.

of an autophagy activator has recently been attempted using a zebrafish model and the beneficial effect of it as well as that of its combination with low-dose rapamycin has been revealed [10]. However, no further studies evaluating autophagy as a new therapeutic target for PKD using other vertebrate models have been conducted.

Herein, we established a rodent model with specific deletion of Ift46 in the renal collecting duct cells. It showed aggressive PKD phenotypes including renal cyst formation as well as abnormally increased proliferating cells around the cyst-lining epithelia. Hyperactivation of mTOR signals followed by inhibition of autophagy flux in *Ift46*-deficient mice was observed. Therefore, we further tried to identify the disease-inhibiting effect of autophagy in PKD. Unexpectedly, neither restoring *LC3* expression nor stimulating autophagy by starvation alleviated the disease progression in both *Ift46*- and *Pkd1*-deleted mice. Enlarged renal cysts and faster renal failure were observed in the groups with enhanced *LC3* expression compared with control mice, and it was markedly confirmed under fasting condition, which induces autophagy *in vivo*. *In vitro* tests revealed that regulation of autophagy either by drugs or by genetic control showed a correlation between Lc3 accumulation and Erk phosphorylation. This disease-accelerating effect of autophagy through stimulation of Erk phosphorylation, suggested the potential negative effect of autophagy on cystogenesis. Moreover, PKD phenotypes were alleviated by an autophagy inhibitor *in vivo*, and the expression profiles of *ATGs* in patients with PKD suggested potential possibilities of using it as a therapeutic target in specific groups of PKD patients.

2. Methods

2.1. Animals

Ift46-targeted JM8A3.N1 ES cell clone (HEPD0687_1_H04) derived from C57BL/6 background was obtained from the EUCOMM and microinjected into C57BL/6J blastocysts, which were then transferred to the uterus of pseudopregnant foster mothers. The original allele derived from the EUCOMM was designated as $Ift46^{tm1a}$. Mice carrying $Ift46^{tm1a}$ allele were crossed with FLPe mice to delete lacZ and neo-cassettes, thereby generating conditional allele $Ift46^{flox}$, wherein exons 5, 6, and 7 were to be excised by Cre in a conditional manner (Fig. S1a-d). We had previously obtained another rodent model, *floxed Pkd1* mice (containing loxP sites flanking exon 2–5 of Pkd1 gene), from Yale University. *HoxB7-Cre* mice were used to generate kidney collecting-duct-specific deletion of either *Ift46* or *Pkd1*. Mice with the genotypes *Ift46 (or Pkd1)* $^{flox/+}$*; HoxB7-Cre* and *Ift46 (or Pkd1)* $^{flox/flox}$*; HoxB7-Cre* were used as controls and experimental animals, respectively. For generation of *mCherry-EGFP-LC3B* transgenic mice, the *mCherry-EGFP-LC3B* construct was amplified from *pBABE-puro mCherry-EGFP-LC3B* (Plasmid #22418, Addgene, MA, USA) using Pfu polymerase and subcloned into the pCAGGS vector with CMV enhancer and chicken β-actin promoter. It was then introduced into the germ line by pronuclear microinjection of fertilized oocytes from C57BL/6J mice and these oocytes were transferred into the oviducts of pseudopregnant foster mothers. Mice aged postnatal 17 days were starved for 24 h to test the effect of autophagy stimulation *in vivo*. These mice had free access to drinking water. All mice were maintained and used following the approval of the Institutional Animal Care and Use Committee (IACUC) at Sookmyung Women's University. Additionally, PKD mice models produced in this work were considered as C57BL/6 strain through SNP panel analysis [11].

2.2. Clinical samples

The study was conducted in accordance with the Declaration of Helsinki and was approved by the Institutional Review Board of Seoul National University Hospital (H-0701-033-195) and Samsung Medical Center (SMC 2019-08-074). Autosomal dominant polycystic kidney disease (ADPKD) and non-ADPKD tissues as paraffin-embedded blocks were obtained from Seoul National University Hospital and Samsung Medical Center, respectively. Mutation types for patients with ADPKD were as follows. One to four PKD cases are PKD1 mutation and the others are unknown, but predicted to be PKD1 mutation. As control, non-cancerous tissues *i.e.*, non-ADPKD tissues in the present study, were obtained from patients with renal cell carcinoma (RCC) who underwent radical nephrectomy.

2.3. Zebrafish models

All zebrafish husbandry and experimental protocols complied with the institutional guidelines were approved by the local ethics board (Sookmyung Women's University Animal Care and Use Committee, SMWU-IACUC-1712-036). Zebrafish were maintained under standard conditions at 28.5 °C with a 14 h light/10 h dark cycle. Embryos were obtained from natural crosses between wild type AB* zebrafish.

2.4. Morpholino and mRNA injections

Morpholinos were designed as described previously [12]: zift46-MO (5′-GGT GCT CTG CTT CTG CCT ACC CGT C-3′) matched to zift46 mRNA from position −25 to −1 relative to the start codon. Morpholino was injected (5–10 nl) into 1–4 cell stage embryos at 1 mM concentration. For lc3 overexpression analyses, full-length lc3 cDNA was synthesised by RT-PCR with total RNA isolated from zebrafish embryos using the following sense (5′-CCA TCG ATT CGA ATT CAT GCC TTC GGA AAA GAC ATT TAA AC -3′) and antisense (5′-GAG AGG CCT TGA ATT CTT ACT GAA ATC CAA ATG TCT CCT GG-3′) primers. Lc3 cDNA was cloned between EcoRI restriction sites of the pCS2+ vector. For *in vitro* transcription, *lc3* RNA was linearized by BamH and synthesized using mMESSAGE mMACHINE™ kit (Ambion). RNAs were microinjected at 100–250 ng/μl concentration in nuclease-free water.

2.5. Cell culture

NIH/3T3 cells (obtained from the Korean Cell Line Bank) were cultured in Dulbecco's modified Eagle medium (DMEM; Welgene, Daegu, South Korea) supplemented with 10% fetal bovine serum (FBS). Mouse inner medullary collecting duct (IMCD) cells were used for analysing cysts *in vitro*. Cells (2.0×10^5 cells/ml) were three-dimensionally cultured in Matrigel (Corning Life Sciences, MA, USA) with DMEM F/12 (Welgene) at 1:1 ratio and additionally cultured in DMEM F/12 with no FBS for 5−6 days.

2.6. Small interfering RNA, plasmids and drugs

Following small interfering RNAs (siRNAs) and plasmids were used. Scrambled siRNA and siRNA targeting *Ift46, Pkd1, Pkd2, Atg5* or *Atg7* (Santa Cruz Biotechnology, Dallas, Texas, USA) were transfected with Lipofectamine RNAiMAX (Invitrogen, Carlsbad, CA, USA). Fugene (Promega, Fitchburg, WI, USA) was used for transfection of plasmids including RFP-GFP-LC3 (Thermo Fisher Scientific, Waltham, MA, USA) and *GFP-tagged Lc3* (OriGene Technologies, Rockville, MD, USA) according to the manufacturer's instructions. Drugs used to regulate autophagy were rapamycin, 3-methyladenine (3-MA), and chloroquine (CQ) (Sigma-Aldrich, St. Louis, MO, USA).

2.7. Histology & immunofluorescence

Tissues were fixed with 4% paraformaldehyde solution, dehydrated in graded ethanol, cleared in xylene, and embedded in paraffin. For histological analysis, sections were counter-stained with haematoxylin and eosin (H&E) and analysed using Olympus microscope and AxioScan (Carl Zeiss, Oberkochen, Germany). Primary antibodies used included acetylated alpha-tubulin (Sigma-Aldrich), rhodamine-conjugated DBA, fluorescein-conjugated DBA, fluorescein-conjugated LTL, Ki-67 (Vector Laboratories, Burlingame, CA, USA), PCNA (Santa Cruz Biotechnology), TUNNEL assay (Roche, USA), Ift46 (Abcam, Cambridge, UK), pErk, pS6R (Cell Signaling Technology, Danvers, MA, USA), and DAPI (Sigma-Aldrich). Secondary antibodies (Santa Cruz Biotechnology) were used to detect primary antibodies. Immunofluorescence images were visualized by confocal microscope (LSM700, Carl Zeiss).

2.8. Western blotting

Total protein was extracted using NucleoSpin RNA/protein isolation kit (Macherey-Nagel, Duren, Germany) and quantified by BCA assay (Sigma-Aldrich). Proteins were separated by SDS-PAGE and transferred onto PVDF membranes. The primary antibodies used were against pMek (S221), Mek, pErk (T202/Y204), Erk, p-S6R (S235/236), S6R, p-Ulk1 (S317), LC3A/B, LC3B, ATG3, ATG5, ATG7, p62 (Cell Signaling Technology), Ift46 (Abcam), Pc1, Pc2 (Santa Cruz Biotechnology) and β-actin (Bethyl Laboratories, Montgomery, TX, USA).

2.9. Microarray data processing

Affymetrix human genome data of GSE7869 and GSE35831 were downloaded from GEO (http://www.ncbi.nlm.nih.gov/geo/) database to profile gene expression levels in whole genome. Affymetrix microarray data were processed according to the workflow of Bioconductor packages (https://bioconductor.org) in R. GSEA (Gene set enrichment analysis) was performed to identify specific functional classes having significantly different gene expression levels between control and PKD tissues [13].

2.10. Statistics

All statistical analyses data are presented as the mean ± standard deviation (S.D.). Student's *t*-test was performed using GraphPad Prism 5.0 (GraphPad software, San Diego, CA, USA). P-values less than 0.05 were considered statistically significant.

3. Results

3.1. Gene expression profiling of autophagy-related genes in human ADPKD

Although autophagy is presumed to be reduced in ADPKD, analysis of the expression pattern of autophagy-related genes in patients with ADPKD has not been reported. Here, we examined the gene expression profile for autophagy regulation using previously published microarray datasets (GSE7869 and GSE35831) derived from human ADPKD samples to confirm whether changes in expression of autophagy-related genes are clinically relevant [14, 15].

In the first dataset (GSE7869), we observed that the positive regulation of 75 autophagy-related genes did not appear to be of clinical relevance in patients with ADPKD (Fig. 1a, b); however, a pattern in which approximately 65% of the altered genes having been increased in ADPKD was found (Fig. 1a-c). Furthermore, the second dataset (GSE35831) also confirmed that the genes positively regulating autophagy were highly and significantly expressed in patients with ADPKD (Fig. 1a, b), suggesting that some patient groups might have increased autophagy in ADPKD.

The expression analysis showed that the expression level of *MAP1LC3B*, which is the coding gene for LC3 protein, did not show a significant difference for ADPKD and control groups at the transcript level, but there seemed to be individual variation among patients with ADPKD (Fig. 1c). To confirm whether this variation pattern of LC3 was observed in patients with ADPKD at the protein level, LC3 protein expression was verified by immunofluorescent staining of cystic tissues. Although LC3 protein was rarely expressed in non-ADPKD tissues, there was a group of patients with ADPKD in which LC3 was strongly expressed (Fig. 1d). These results suggest that decreased autophagy cannot be considered as a general feature of ADPKD patients; therefore, we tried to further investigate the precise link between autophagy and PKD progression using the newly established PKD mice model. Loss of Ift46 in the renal collecting duct causes PKD accompanied by ciliary defects and hyper-activates MAPK/Erk and mTOR pathways.

3.2. Loss of Ift46 in the renal collecting duct causes PKD accompanied by ciliary defects and hyper-activates MAPK/Erk and mTOR pathways

Floxed allele of *Ift46* was created and HoxB7-Cre mice were used to delete Ift46 in the renal collecting duct cells. Mice with *HoxB7-Cre* transgene highly express Cre recombinase in the ureteric bud that develops into the renal collecting duct [16]; therefore, HoxB7-Cre specifically inactivates Ift46 in the renal collecting duct. At postnatal day (p) 5, modest dilation and small cysts were observed, and by p10 to p21, fluid-filled cysts of varying sizes, mostly originating from the collecting ducts, were observed in kidneys of *Ift46*-deficient mice (Fig. 2a-c). Blood urea nitrogen (BUN) levels and the ratio of the weight of the two kidneys (2KW) to the total body weight (TBW) dramatically increased in *Ift46*-deficient kidneys at p10 and p21, indicating renal dysfunction (Fig. 2d, e). Consistent with the renal failure, fibrotic cystic kidney accompanied by collagen accumulation was observed in *Ift46*-deficient mice (Fig. 2f). Moreover, absence of primary cilia was observed in renal collecting duct cells of *Ift46*-deficient mice, suggesting that *Ift46* deletion led to polycystic kidneys with cilia loss (Fig. S1e, f). As dysregulated cell proliferation and apoptosis are key phenotypes of PKD [17-19], we next confirmed whether *Ift46* has an effect on the alteration of cell proliferation and apoptosis. Increased signals of proliferation markers (Ki-67 and PCNA) and apoptosis marked by TUNEL-positive cells were observed in the cystic kidneys at p21 (Fig. 2g). To clarify the altered signaling pathways

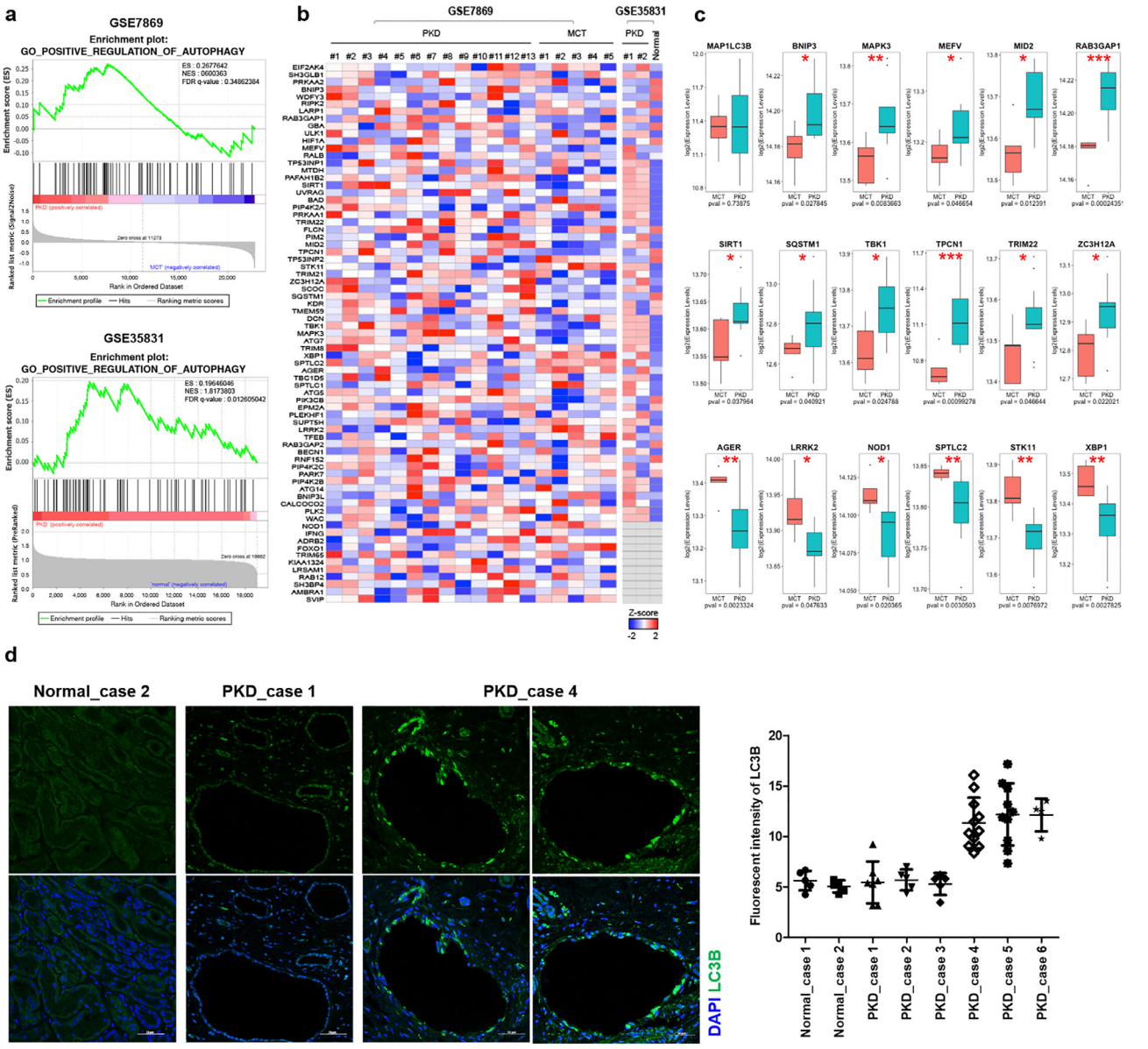

Fig 1. Validation of autophagy-related genes in the kidneys of patients with ADPKD.

(a) Gene set enrichment analysis of 75 autophagy-related genes between ADPKD and control groups. (b) Heatmaps of genes that are from Fig. 1a. in each sample. (c) Expression levels of *MAP1LC3B* and other significantly altered genes from GSE7869 involved in positive regulation of autophagy. Statistical analysis performed using t-tests, and $P < 0.05$ was considered statistically significant ($^{*}P < 0.05$, $^{**}P < 0.01$, $^{***}P < 0.001$). (d) Immunofluorescent staining of human kidney tissues with or without PKD for LC3B. Fluorescence intensity of the signals was quantified by green histogram analyses using Image J program.(For interpretation of the references to color in this figure legend, the reader is referred to the web version of this article.)

involved in cyst formation in the *Ift46*-deleted kidneys, the expression of MAPK/ERK and mTOR pathways was evaluated. Kidneys of *Ift46*-deficient mice at p21 showed hyper-activated MAP kinases and mTOR in the collecting duct-specific cyst-lining epithelia as well as whole kidney lysates compared with those from control mice (Fig. 2h-j). These observations suggest that activation of MAPK/ERK and mTOR pathways is involved in renal cystogenesis induced by *Ift46* deficiency.

3.3. *Cyst development is accelerated in Ift46-deficient mice with enhanced LC3 expression under autophagy induction* in vivo

mTOR is a key negative regulator of autophagy; therefore, we screened for a basal autophagy level by checking the expression of multiple autophagy-related proteins (Atgs) in *Ift46*-deleted mice kidneys. Atgs were reduced in *Ift46*-deleted kidneys, indicating that basal autophagy was inhibited (Fig. 3a). We next monitored the changes in autophagy flux after 1-day starvation to confirm whether autophagy functions properly in the *Ift46*-deleted model. Unc-51 like autophagy activating kinase 1 (Ulk-1) and p62 were used as markers. During autophagy, Ulk-1 is accumulated and plays a central role in the initial stage of autophagy, while p62 is itself an autophagy substrate, therefore is finally degraded at the end of the process. Ulk-1 activation and lowered p62 upon 1-day starvation were normally observed in wild type (Left). However, Ift46-deleted mice kidneys (Right) failed to properly induce autophagy, indicating that autophagy is dysregulated in *Ift46*-deleted kidneys (Fig. 3b).

To test the therapeutic effect of autophagy *in vivo*, we crossed heterozygous *Ift46f* mice with *LC3* transgenic mice (Fig. 3c). LC3 plays a key role in autophagy, in regulating autophagosome membrane expansion and fusion with lysosomes. Therefore, we hypothesized that LC3 overexpression could enhance autophagy in *Ift46*-deleted

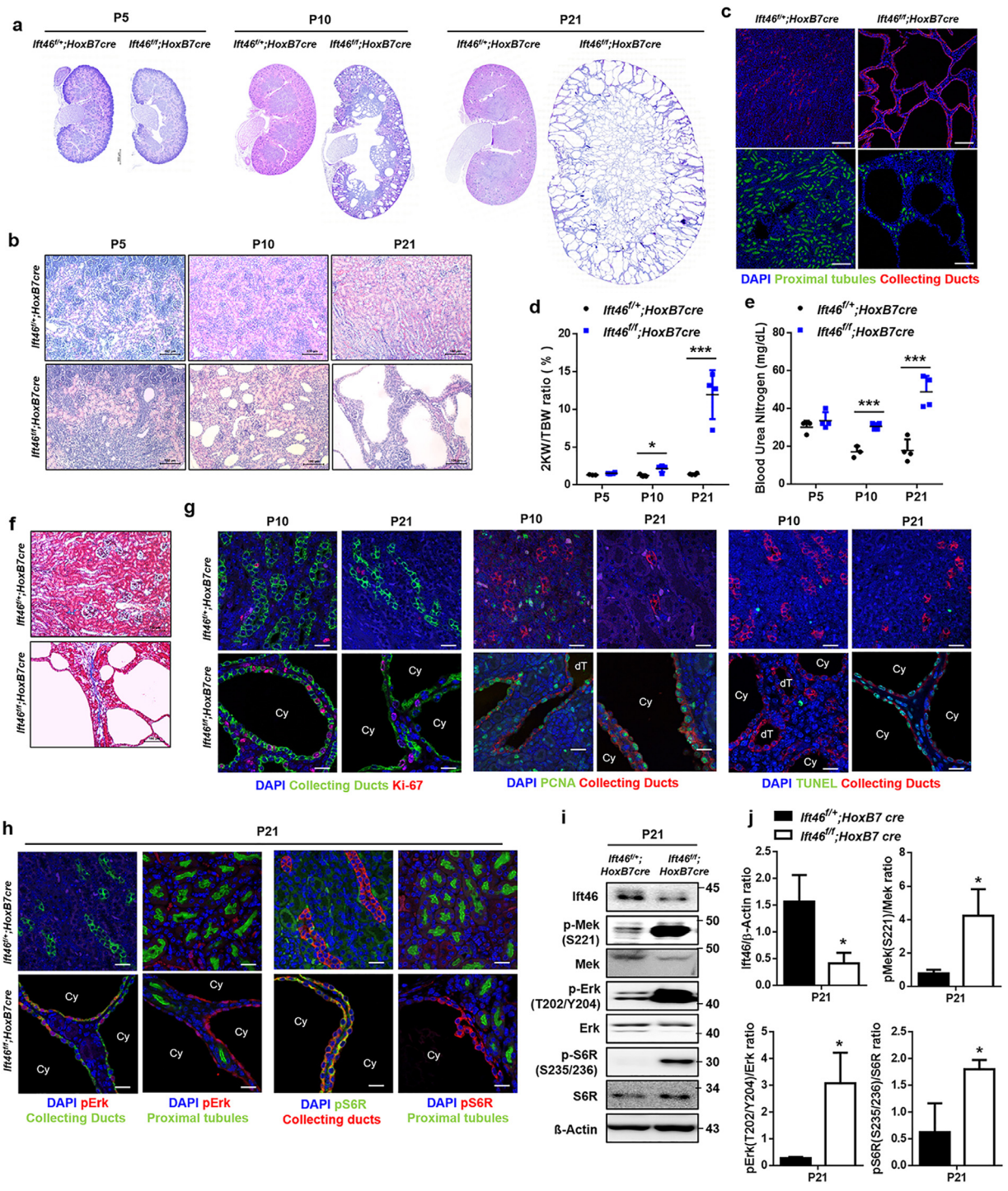

Fig 2. Renal cystic phenotypes with mTOR hyper-activation in Ift46-deleted mice.

(a) Haematoxylin and eosin (H&E)-stained sections of *Ift46*$^{flox/+}$*; HoxB7-Cre* and *Ift46*$^{flox/flox}$*; HoxB7-Cre* kidneys at p5, p10, and p21. Scale bar, 500 μm. (b) High magnification image of H&E-stained sections of *Ift46*$^{flox/+}$*; HoxB7-Cre* and *Ift46*$^{flox/flox}$*; HoxB7-Cre* kidneys at p5, p10, and p21. Scale bar, 100 μm. (c) The kidneys of *Ift46*$^{flox/+}$*; HoxB7-Cre* and *Ift46*$^{flox/flox}$*; HoxB7-Cre* mice (p21) stained with markers for collecting ducts (red), proximal tubules (green) and nuclei (DAPI, blue). Scale bar, 100 μm. (d) Ratio of the weight of two kidneys (2KW) to the total body weight (TBW) of *Ift46*$^{flox/+}$*; HoxB7-Cre* and *Ift46*$^{flox/flox}$*; HoxB7-Cre* mice at p5, p10, and p21. Data are shown as mean ± SD; $n \geq 3$ for each time point; $^{*}p < 0.05$, $^{***}p < 0.005$. (e) Blood urea nitrogen (BUN) levels in the kidneys of *Ift46*$^{flox/+}$*; HoxB7-Cre* and *Ift46*$^{flox/flox}$*; HoxB7-Cre* mice at p5, p10, and p21. Data are shown as mean ± SD; $n \geq 3$ for each time point; $^{***}p < 0.005$. (f) Masson's trichrome staining of kidney sections of *Ift46*$^{flox/+}$*; HoxB7-Cre* and *Ift46*$^{flox/flox}$*; HoxB7-Cre* kidneys at p21. Scale bar, 100 μm. (g) Kidneys of *Ift46*$^{flox/+}$*; HoxB7-Cre* and *Ift46*$^{flox/flox}$*; HoxB7-Cre* mice (p10, p21) stained with markers for collecting duct (green or red), Ki-67 (red), PCNA (green), TUNEL (green) and nuclei (DAPI, blue). Scale bar, 20 μm. (h) Kidneys of *Ift46*$^{flox/+}$*; HoxB7-Cre* and *Ift46*$^{flox/flox}$*; HoxB7-Cre* mice were stained for collecting ducts (green or red), proximal tubules (green), pS6R (green or red), pErk (red) and nuclei (DAPI, blue) at p21. Scale bar, 20 μm. (i) Western blot analysis of MAPK/ERK and mTOR signaling using whole kidney lysates of *Ift46*$^{flox/+}$*; HoxB7-Cre* and *Ift46*$^{flox/flox}$*; HoxB7-Cre* mice at p21. (j) Quantification of band intensity observed in panel (i). Data are shown as mean ± SD; $n \geq 3$ for each time point; $^{*}p < 0.05$.(For interpretation of the references to color in this figure legend, the reader is referred to the web version of this article.).

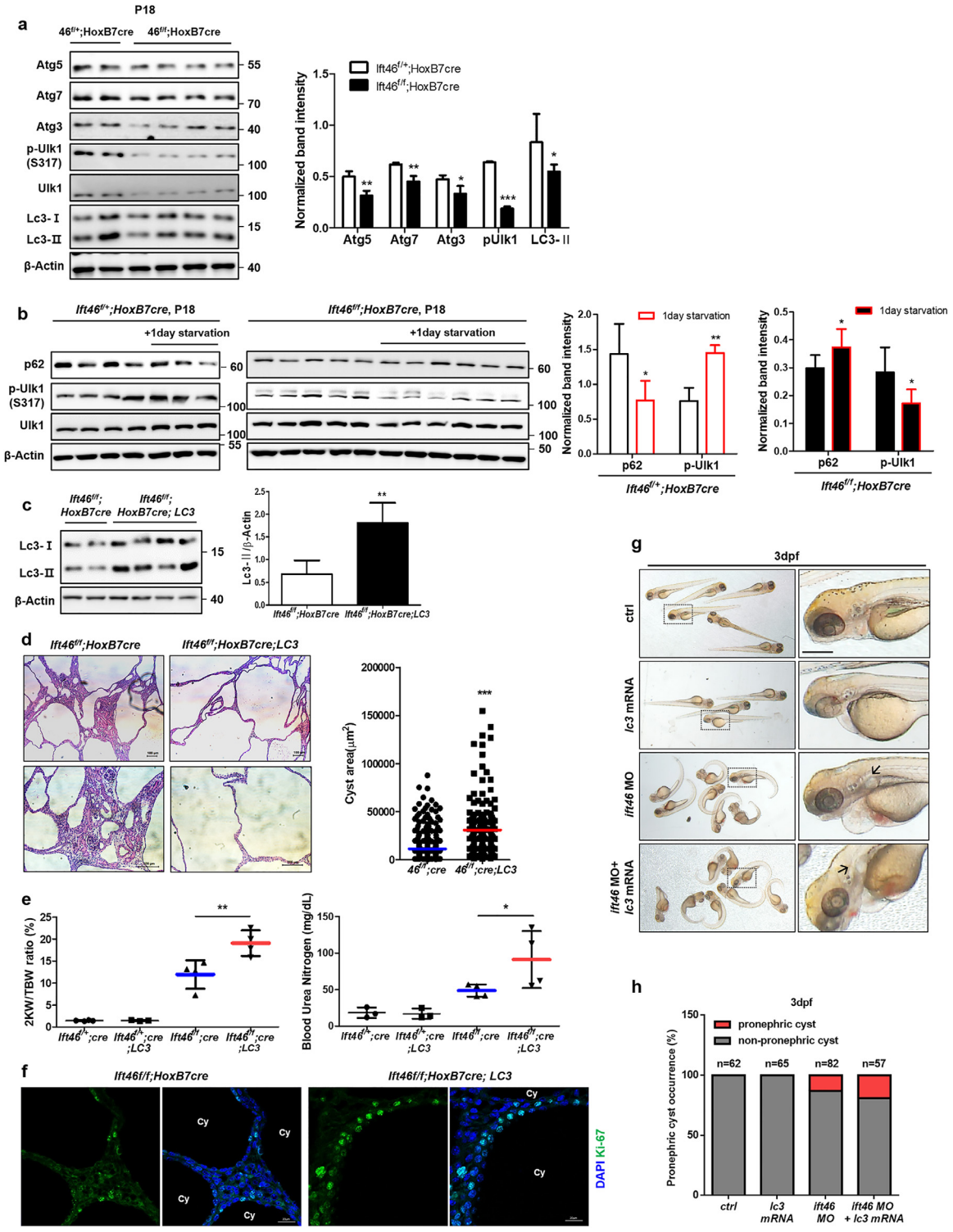

Fig 3. Accelerated renal cyst development with reduced renal function in *LC3*-overexpressed *Ift46*-deleted models.

(a) Reduced expression of autophagy-regulating proteins including Atg5, Atg7, Atg3, p-Ulk1 (S317) and Lc3 in *Ift46*$^{flox/flox}$*; HoxB7-Cre* mice. (b) Inhibited autophagy flux upon 1-day starvation in *Ift46*$^{flox/flox}$*; HoxB7-Cre* mice. (c) The protein expression level of Lc3 in *Ift46*$^{flox/flox}$*; HoxB7-Cre; Lc3*. (d) Haematoxylin and eosin (H&E)-stained sections of *Ift46*$^{flox/flox}$*; HoxB7-Cre; Lc3* mice at p21. Scale bar, 100 μm. Cyst area was quantified by Image J program. Data are shown as mean ± SD. (e) Ratio of the weight of two kidneys (2KW) to the total body weight (TBW) and blood urea nitrogen (BUN) level of *Ift46*$^{flox/flox}$*; HoxB7-Cre* mice at p21. (f) Staining of cystic kidney tissues of *Ift46*$^{flox/flox}$*; HoxB7-Cre* mice with or without *Lc3* overexpression for Ki-67 to reveal changes in cell proliferation. Scale bar, 20 μm. Data are shown as mean ± SD; $n \geq 3$ and $P < 0.05$ was considered statistically significant (* $P < 0.05$, ** $P < 0.01$, *** $P < 0.001$). (g) Zebrafish embryos injected with indicated morpholino (MO) and *lc3* mRNA at 3 dpf. Arrows indicate pronephric cysts. Scale bar, 0.3 mm. (h) Graph showing occurrence of pronephric cysts in indicated groups.

mice kidneys, which show altered autophagy flux. However, significant increase in the renal cystic volume (Fig. 3d) and faster renal dysfunction were unexpectedly observed in the *LC3*-overexpressed group compared with control group (Fig. 3e). In addition, fluorescence immunohistochemistry data showed increased cell proliferation in the kidneys of homozygous Ift46 mice with enhanced LC3, specifically around the cyst-lining cells (Fig. 3f). To confirm whether these phenotypic changes also occur in another *in vivo* model, we injected *lc3* mRNA into zebrafish *ift46* morphants showing pronephric cyst phenotype [20]. Co-injection of *ift46* morpholino (MO) and *lc3* mRNA increased pronephric cyst occurrence compared with that in *ift46* morphants (Fig. 3g, h). These data show that *lc3* overexpression in zebrafish *ift46* morphants are phenotypically similar to *Ift46* mice, which indicate that LC3 overexpression accelerates cyst formation *in vivo* PKD models.

3.4. Autophagy induction (via starvation) leads to faster renal dysfunction, which was rescued by 3-MA treatment in Ift46-deleted mice

To further investigate the role of autophagy activation in cystogenesis *in vivo*, mice were starved for 24 h starting at 17 days after birth to stimulate autophagy (Fig. 4a). As a result, LC3 was significantly activated upon 1d starvation and renal function was highly reduced with enlarged cysts upon starvation, especially in *LC3*-overexpressed *Ift46*-deleted mice (Fig. 4b, c). *Ift46$^{f/f}$; HoxB7cre* mice also showed an increase in kidney volume and BUN level, indicating the effect of full day starvation at p17, which is over 5% of their life. However, the changes in 2KW/TBW ratio and BUN level were higher in *LC3*-overexpressed group (Fig. 4b). H&E stained sections also revealed a significant increase in cyst area under autophagy stimulation both in *Ift46$^{f/f}$; HoxB7cre* and *Ift46$^{f/f}$; HoxB7cre; LC3* mice (Fig 4d). Next, we intraperitoneally administered 3-MA, an autophagy inhibitor involved in the early stage of autophagy, to identify the effect of autophagy inhibition. Mice were injected with either PBS or 3-MA twice on the 15th and 16th day after birth, and sacrificed 1 day after starvation for autophagy induction (Fig. 4e). The 3-MA-treated *Ift46$^{f/f}$; HoxB7cre; LC3* mice showed decreased LC3 activation and a lower 2KW/TBW ratio, as well as improved renal function compared to the PBS-treated mice (Fig. 4f, g). In addition, fluorescent immunohistochemistry analysis showed that LC3 expression around the cysts was highly reduced in the experimental group compared to the control group (Fig. 4h). And cyst area was highly decreased in 3-MA injected groups both of *Ift46$^{f/f}$; HoxB7cre* and *Ift46$^{f/f}$; HoxB7cre; LC3* mice (Fig 4i). These findings, wherein PKD phenotypes were accelerated by the induction of autophagy and rescued by an autophagy inhibitor, were contrary to what we had expected; therefore, the specific mechanisms underlying the stimulation of cyst development by LC3 were further evaluated.

3.5. Phosphorylation of ERK is positively regulated by LC3 under autophagy induction

A recent study has elucidated the positive regulatory mechanisms of LC3-stimulated activation of ERK and its signaling cascades under exposure to growth factors. Moreover, ERK cascade molecules, including MEK, are localized to the cytoplasmic side of autophagosomes and LC3 positively regulates their activation through direct physical interaction with them [21]. Hyper-activated ERK after cAMP accumulation is one of the well-understood aberrant signaling pathways in PKD; therefore, we next identified the role of LC3 in increasing ERK activation and its involvement in the pathogenesis of PKD under autophagy induction. Rapamycin, an inhibitor of mTOR, was used for *in vitro* analyses to stimulate autophagy, which was successfully confirmed by both LC3-GFP detection and puncta of autophagosomes fused with lysosomes (Fig. 5a). Phosphorylation of Erk was enhanced with increased Lc3 activation in response to rapamycin treatment (Fig. 5b). In addition, two autophagy inhibitors, 3-MA and CQ, were used to further investigate the correlation between Lc3 and Erk phosphorylation. These drugs differentially inhibit autophagy, such that 3-MA blocks autophagosome formation through class III PI3K, and CQ prevents autophagosome-lysosome fusion, thereby accumulating autophagosomes. With different intracellular Lc3 expression, remarkably hyper-activation of Erk with accumulation of Lc3 by CQ was observed, while 3-MA inhibited Erk phosphorylation as well as Lc3 (Fig. 5c). Overexpression of *Lc3* itself did not show apparent changes, while treatment with rapamycin increased phosphorylated Erk levels (Fig. 5d). To confirm how ATG alterations affected Erk activation, we silenced *Atg5* and *Atg7* under treatment with either DMSO or rapamycin. Lc3 activation was highly reduced in *Atg*-silenced cells, particularly under autophagy stimulation, and it further inhibited Erk phosphorylation (Fig. 5e).

3.6. Similar effects of Lc3 overexpression and autophagy stimulation were observed in the PKD1-targeting model

We performed a three-dimensional (3D) culture to evaluate the effect of *Lc3* overexpression followed by enhanced Erk activation on *in vitro* cysts induced by *Ift46*-silencing. Transfected cells with siRNA targeting *Ift46* and/or *Lc3* were embedded in Matrigel, and were observed 5–6 days after seeding. *In vitro* cysts were gradually formed after 2–3 days of seeding, and larger cysts were observed with *Ift46* deficiency compared with control. Furthermore, average cystic area was highly increased in *Ift46*-knockdown cells with enhanced *Lc3* expression (Fig. 6a, c).

Pkd1 and *Pkd2* are the main causative genes of PKD; therefore, we wondered whether Lc3 could also stimulate cysts derived from PKD gene deficiencies. As observed in *Ift46*-silenced cells, *in vitro* cysts were stimulated by *Pkd1*- or *Pkd2*-silencing, and further increased by *Lc3* overexpression only in *Pkd1*-silenced cells (Fig. 6a, c). Erk phosphorylation was also enhanced by *Lc3* overexpression in each group with gene deficiencies (Fig. 6b).

To confirm the effect of *LC3* overexpression on *in vivo* renal cysts originating from mice with *Pkd1* deletion, we used a collecting duct-specific *Pkd1*-deleted mouse model. *Pkd1*-targeted mice showed radical and more severe progression with shorter lifespans compared with that shown by *Ift46*-targeted mice. Furthermore, the mice were starved for 24 h starting from 12 days after birth followed by sacrifice at postnatal day 13. As a result, *Pkd1*-knockout mice with enhanced LC3 led to end-stage renal disease (ESRD) earlier than control mice (Fig. 6d). Immunofluorescence data revealed that phosphorylated ERK was highly detected around the cyst-lining cells in kidneys of *Pkd1*-deleted *LC3*-overexpressed mice (Fig. 6e). These findings indicate that the negative effects of LC3, including increased Erk phosphorylation and enlarged cysts observed in *Ift46*-deficient mice, were not limited to a specific PKD model.

Collectively, we observed highly variable expression profiles of ATGs in patients with ADPKD using two different microarray datasets. They contradicted previous studies hypothesizing reduced autophagy levels in PKD. We next observed that basal autophagy was generally decreased, with mTOR hyper-activation in collecting duct-specific *Ift46*-deleted mice. When autophagy was enhanced in *LC3* transgenic mice, more enlarged cysts with reduced renal function appeared unexpectedly, which further worsened under autophagy induction. It was then partially alleviated by autophagy inhibition, suggesting potential possibilities for therapeutic use of autophagy inhibitors in specific groups of patients with PKD. Similar results were observed in *Pkd1*-deleted model, indicating that autophagy stimulation might accelerate the disease regardless of the target genes.

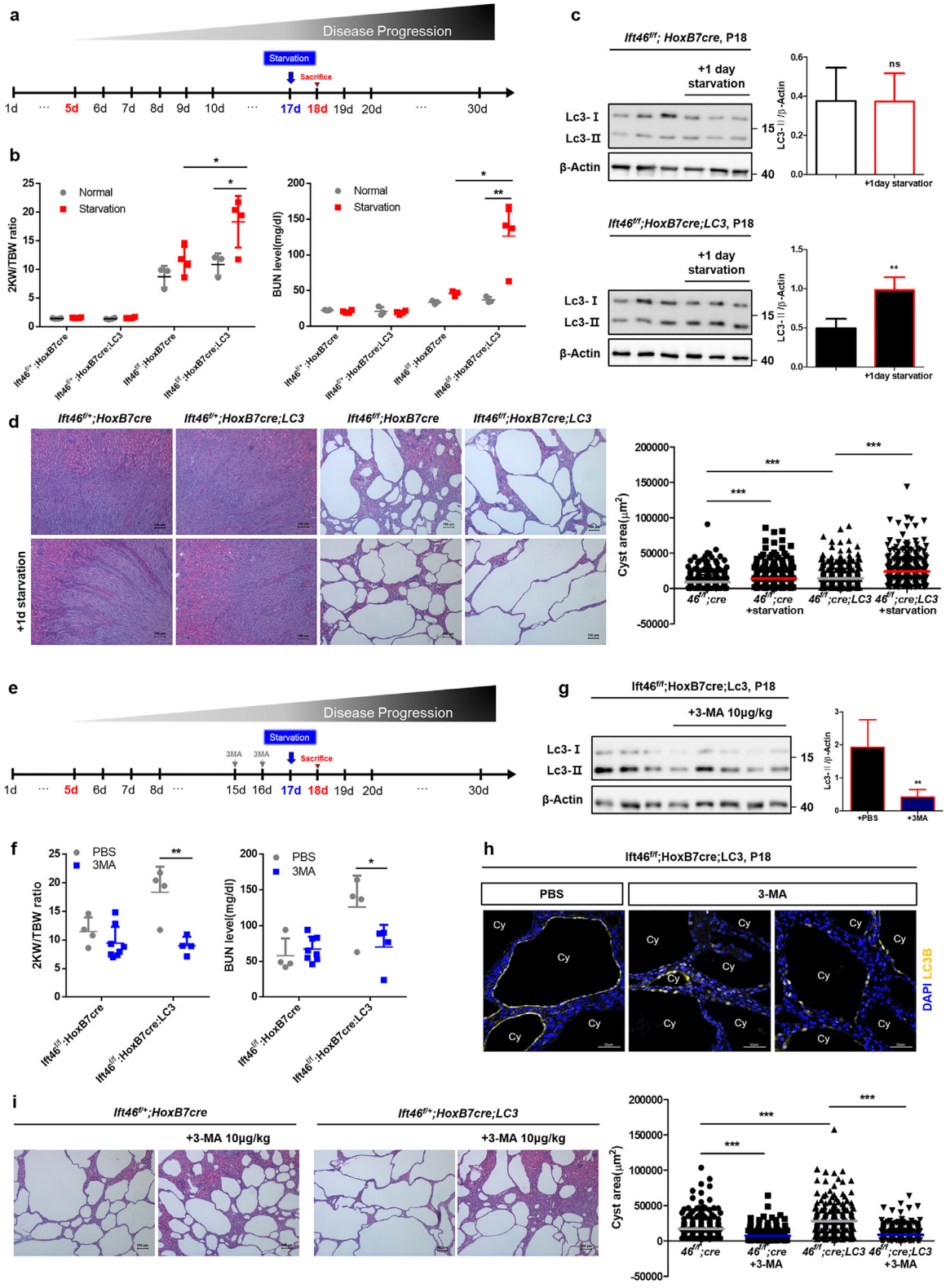

Fig 4. Increased growth of renal cysts upon stimulation of autophagy in *Ift46*-targeted mice and rescued by 3-methyladenine.

(a) Schedule for starving mice to stimulate autophagy in *Ift46*$^{flox/flox}$; *HoxB7-Cre* mice with or without *Lc3* overexpression. (b) Testing renal function based on the ratio of the weight of two kidneys (2KW) to the total body weight (TBW) and blood urea nitrogen (BUN) level. (c) Immunoblotting analysis shows changes in Lc3 level in *Ift46*$^{flox/flox}$; *HoxB7-Cre* mice with or without *Lc3* overexpression after 1-day starvation. (d) Haematoxylin and eosin (H&E)-stained sections of *Ift46*$^{flox/flox}$; *HoxB7-Cre* mice with or without *Lc3* overexpression after 1-day starvation. Scale bar, 100 μm. Cyst area was quantified by Image J program. Data are shown as mean ± SD. (e) Schedule for 3-methyladenine (3-MA) injection into *Ift46*$^{flox/flox}$; *HoxB7-Cre* mice with or without *Lc3* overexpression. (f) Change in the 2KW/TBW ratio and BUN level. (g) Reduced Lc3 level in *Ift46*$^{flox/flox}$; *HoxB7-Cre; Lc3* mice injected with 3-MA. (h) Expression and localization of LC3 in cystic renal tissues of control or experimental groups. Scale bar, 50 μm. (i) H&E-stained sections of *Ift46*$^{flox/flox}$; *HoxB7-Cre* mice with or without *Lc3* overexpression upon 24 h starvation after 3-MA injection. Scale bar, 100 μm. Cyst area was quantified by Image J program. Graphs represent data as mean ± SD; $n \geq 3$ for each group and $P < 0.05$ was considered statistically significant (* $P < 0.05$, ** $P < 0.01$, *** $P < 0.001$). .

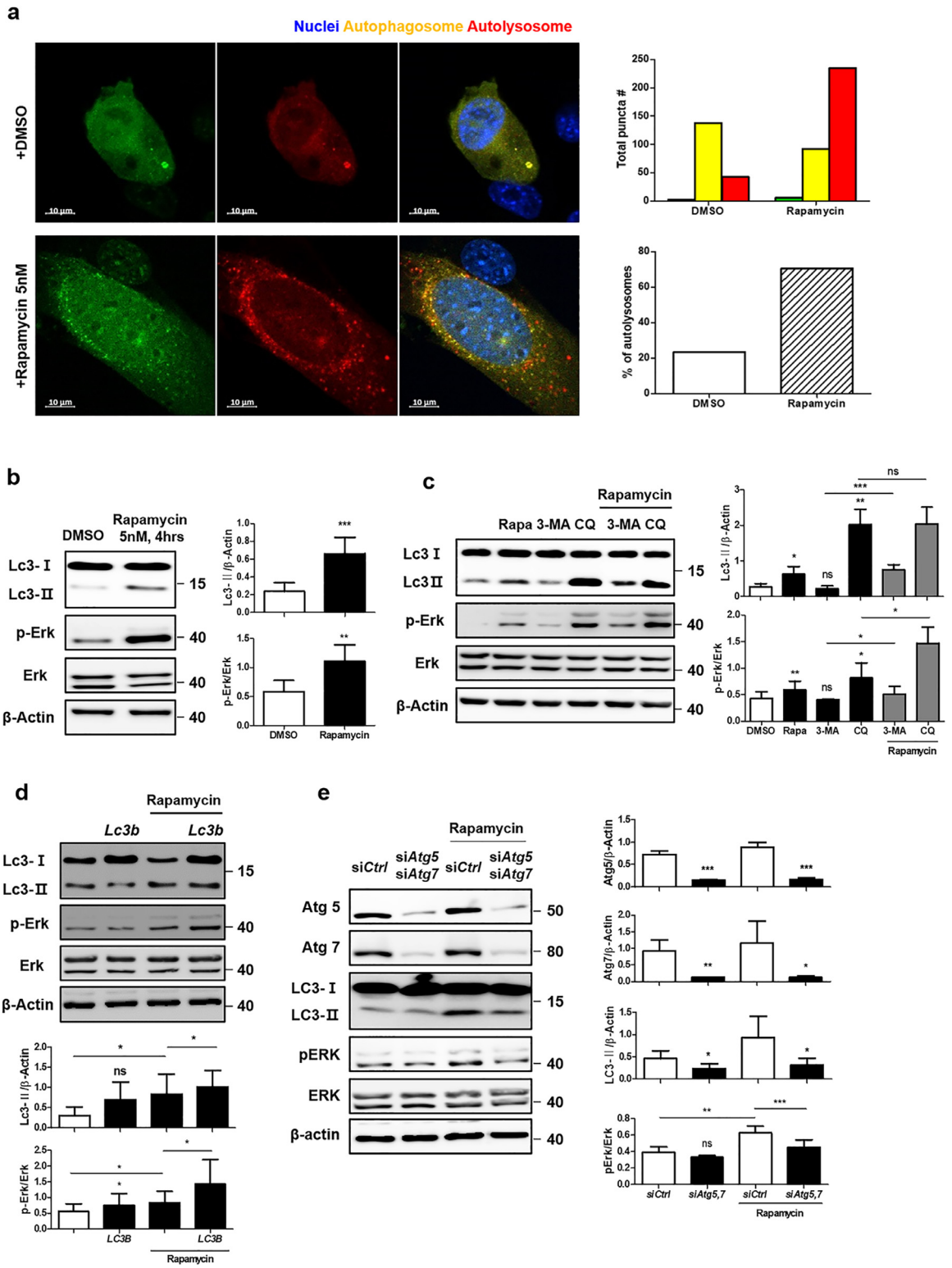

Fig 5. Positive regulation of Erk activation by Lc3 and its effect on *in vitro* cystogenesis.

(a) Ratio of autophagosomes fused with lysosomes after 5 nM rapamycin treatment for 4 h. Scale bar, 10 μm. (b) Change in Erk phosphorylation with 5 nM rapamycin treatment for 4 h. (c) Effect of autophagy inhibitors including 3-methyladenine (3-MA) (1 mM) and chloroquine (CQ) (50 μM) on Erk phosphorylation. (d) Increase in Erk phosphorylation in *Lc3*-overexpressed cells with rapamycin treatment (5 nM, 4 h). (e) Decrease in Erk phosphorylation in *Atg5*- and *Atg7*-silenced cells with rapamycin treatment. All data were obtained from a minimum of three independent experiments. Statistical analysis performed using one-tailed t-tests, and $P < 0.05$ was considered statistically significant (* $P < 0.05$, ** $P < 0.01$, *** $P < 0.001$).

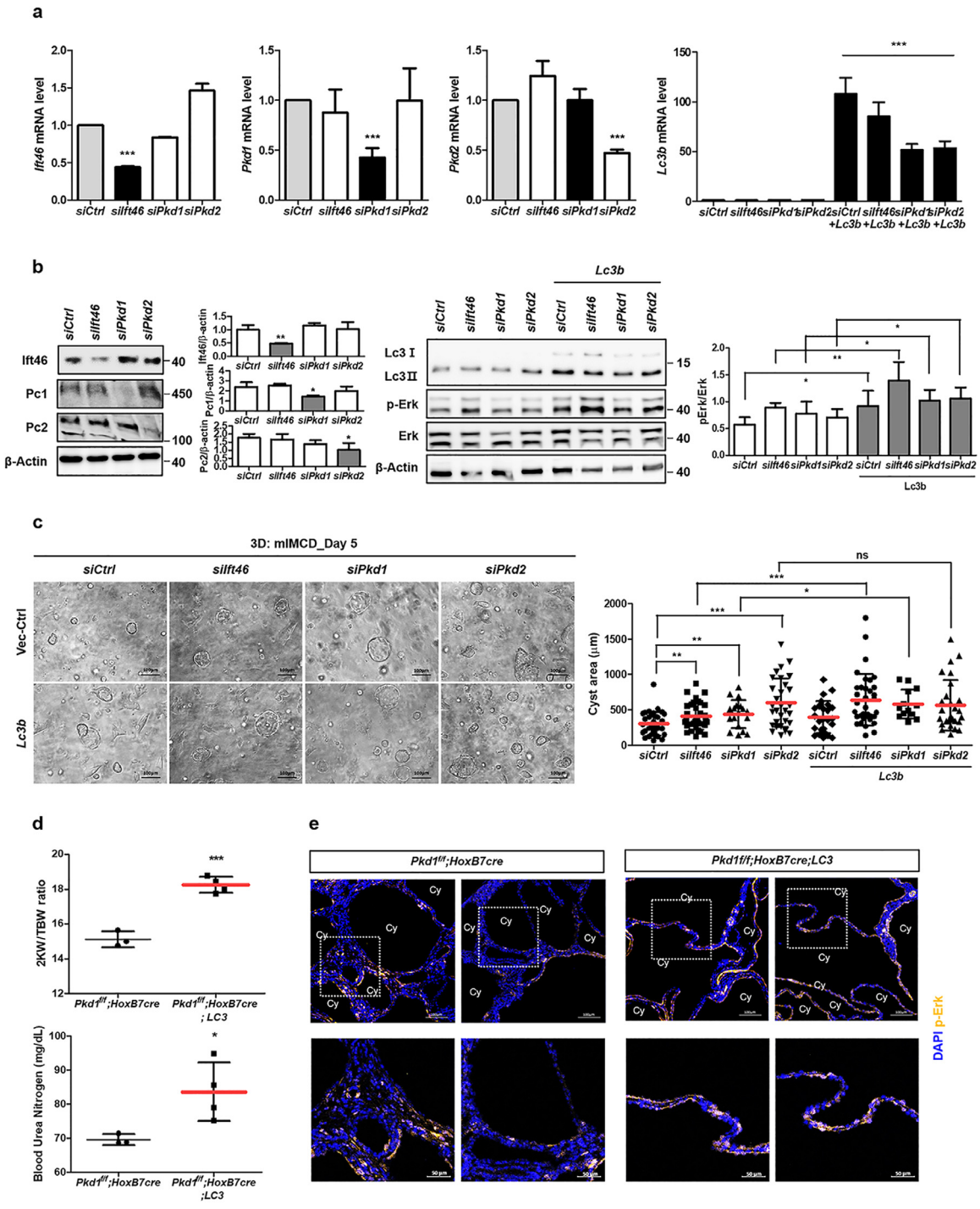

Fig 6. Effect of *Lc3* overexpression on cysts *in vitro* and in *Pkd1*-targeted mice.

(a) Screening of mRNA expression level after transfection of *Ift46* siRNA, *Pkd1* siRNA, *Pkd2* siRNA or *Lc3*. (b) Changes in expression of the proteins including Ift46, Pc-1, Pc-2, and Lc3 and Erk phosphorylation. (c) Cysts observed by *in vitro* 3D culture after increasing Lc3 expression and counts of *in vitro* cystic area for each group. Graphs represent data as mean ± SD; $n > 20$ for each group. (d) Changes of the ratio of the weight of two kidneys (2KW) to the total body weight (TBW) and blood urea nitrogen (BUN) level in $Pkd1^{flox/flox}$; *HoxB7-Cre; Lc3* mice. (e) Fluorescent staining of phosphorylated Erk in kidney tissues. Lower panels are enlarged from upper ones. Scale bar, 100 μm for images with high magnification and 50 μm for zoom-in images. Graphs represent data as mean ± SD; $n \geq 3$ for each group and $P < 0.05$ was considered statistically significant (* $P < 0.05$, ** $P < 0.01$, *** $P < 0.001$).

4. Discussion

Recently, several studies have shown dysregulated autophagy in disease models of ciliary defects and *vice versa*, indicating a strong association between autophagy and ciliogenesis [22]. One of them was PKD in which multiple renal cysts appear by germline mutations of ciliary proteins. There are several reasons why many researchers are particularly interested in autophagy dysregulation in PKD. First, mTOR, a key negative regulator of autophagy, is commonly hyperactivated and has been considered as a therapeutic target for PKD. Indeed, specific inhibitors targeting mTOR signals including rapamycin, metformin, and curcumin have attenuated disease phenotypes with autophagy stimulation in PKD mice [23, 24]. Therefore, a recent study has attempted to identify the therapeutic benefits of autophagy

activation in PKD by directly targeting autophagy with a specific inducer [10]. In addition, they used a combination treatment comprising ten-fold lower doses of rapamycin and an autophagy activator on a *pkd1*-mutated zebrafish model. The combination treatment indeed reduced the cyst growth by almost the same level as that by rapamycin alone at higher doses, suggesting new therapeutic strategies with potentially reduced drug toxicity in PKD while targeting mTOR.

Herein, we attempted to further evaluate the precise role of autophagy in PKD progression. We established a new mouse model with loss of Ift46, specifically in the renal collecting duct cells via a cre-loxp system. The collecting duct-specific *Ift46*-knockout mice showed loss of cilia and severe polycystic kidney phenotype with hyper-activation of MAP kinases and mTOR, and short lifespans of approximately less than a month.

We next hypothesized that increase in autophagy via enhanced expression of a key autophagy modulator could slow the disease progression. Prior to testing its therapeutic effects, we screened the basal autophagy level in *Ift46*-deficient mice and found it to be reduced in polycystic kidneys. *Lc3* transgenic mice were thought to have restored autophagy levels; however, neither restoring *Lc3* expression nor autophagy stimulation alleviated PKD. Moreover, it further led to progression towards the end-stage renal disease (ESRD) earlier with more enlarged cysts. *In vitro* tests including drugs treatments, silencing of autophagy genes, and analysis of *in vitro* cysts via 3D culture system, markedly revealed the positive regulation of Erk by LC3. In particular, 3-MA treatment, which initially inhibited LC3 activation, showed reduced Erk activation, and it finally alleviated PKD pathologies.

Autophagy is reported to be reduced in PKD mice models; therefore, autophagy activation is suggested as one of the potential therapeutic strategies. Starvation is the most reliable physiological inducer of autophagy in mice, and a previous study by Warner et al. had demonstrated the beneficial effect of food restriction (FR) in PKD mice. Six-week-old mice were starved by a decrease of 30−50% of total caloric intake for six months. They showed reduced cyst growth, renal fibrosis, inflammation and injuries; however, no significant changes in autophagy were observed [25]. This may indicate that mild to moderate FR did not successfully induce autophagy, thereby a specific effect of autophagy stimulation on PKD progression could not be observed. Therefore, our findings from rapid fasting conditions may suggest the cyst-stimulating effect of autophagy. Moreover, autophagy is generally expected to be reduced in patients with PKD; however, our clinical data revealed that the expression of ATGs including *LC3B* varies from case to case. Therefore, while our findings support the possible therapeutic use of autophagy inhibitors in a specific group of patients with altered autophagy, they should be considered with caution. The disease onset patterns are highly different between PKD patients and animal models of PKD. In human PKD, the age at which end-stage renal disease (ESRD) occurs is highly variable, but in most cases, it is observed post 50 years of their life though the genetic mutation is present at birth. On the contrary, severe and rapid development of phenotypes is observed in rodent models with mutation in *Pkd1, Pkd2,* or other ciliary genes. They display embryonic lethality or short lifespans of less than a month. Therefore, there are limitations to the direct application of mTOR inhibitors to patients based on the observations in preclinical models. Indeed, a number of other preclinical studies had developmental issues. mTOR inhibitors, including rapamycin, sirolimus, and everolimus, were previously reported to markedly reduce cyst growth with delayed loss of renal function in Han; SPRD rat model [26-28]. In particular, sirolimus also showed partial therapeutic effects in Pkd2WS25/- mice, an ortholog of the human ADPKD model, indicating its potential to be applied to clinical studies [24]. Based on the remarkable cyst-inhibiting effect of mTOR-targeting drugs observed in rodent models, large randomized clinical trials have been conducted; however, they revealed insignificant changes in total kidney volume (TKV) on MRI [29, 30]. This was attributed to the limited doses permitted for clinical trials as well as low tissue specificity. To overcome these limitations, new strategies such as those applying a conjugated form, which enhances the ability of drugs to reach kidneys more efficiently, were generally explored in more recent studies [31]. Similarly, our findings might provide another evidence to explain the limited therapeutic effects of mTOR inhibition in PKD patients, and suggest potential possibilities of autophagy inhibitors as therapeutic agents. Finding ways to overcome discrepancies in PKD onset patterns between humans and animals may be critical to increase the possibility of applying candidate targets. In addition, new strategies to enhance the efficiency or specificity of the drugs should be considered to further advance PKD therapy.

Contributors

J.H. Park and G.T. Oh designed the study; E.J. Lee and J.Y. Ko analysed *in vivo* phenotypes, conducted autophagy experiments, and wrote manuscript; E.J. Lee, J. Joen and H. Mun conducted *in vitro* tests; C.J. Lim and S.W. Seo generated Ift46 flox mice; K.H. Yoo and S. Oh analysed gene expression profiles using microarray datasets; H. Kim, Y.K. Oh, C. Ahn, and M.Y. Kang discussed the data on clinical samples; M.J. Kim generated zebrafish models targeting either Ift46 or LC3; H.W. Ko discussed ciliopathy models.

Funding sources

This work was supported by grants from the Bio & Medical Technology Development Program [2015M3A9B6027555]; the Collaborative Genome Program for Fostering New Post-Genome Industry of the NRF [2014M3C9A2067613]; the Basic Science Program [2016R1A5A1011974 and 2019R1A2B5B03069738]. The funders of the study had no role in the study design, data collection, data analysis, data interpretation, or writing of the report.

Declaration of Competing Interest

J.H. Park, G.T. Oh and J.Y. Ko have filed a patent in South Korea for the establishment of the Ift46-deleted model (patent number: 10-1618124). The others have nothing to disclose.

Acknowledgments

We thank Dr. S. Somlo (Yale University) for the $Pkd1^{flox/flox}$ mice and Dr. M. Shong (Chungnam National University) for HoxB7-Cre transgenic mice.

Supplementary materials

Supplementary material associated with this article can be found, in the online version, at doi:10.1016/j.ebiom.2020.102986.

References

[1] Nauli SM, Zhou J. Polycystins and mechanosensation in renal and nodal cilia. Bioessays 2004;26(8):844–56.
[2] Harris PC, Torres VE. Polycystic kidney disease. Annu Rev Med 2009;60:321–37.
[3] Nauli SM, Alenghat FJ, Luo Y, Williams E, Vassilev P, Li X, et al. Polycystins 1 and 2 mediate mechanosensation in the primary cilium of kidney cells. Nat Genet 2003;33(2):129–37.
[4] Torres VE, Harris PC. Strategies targeting cAMP signaling in the treatment of polycystic kidney disease. J Am Soc Nephrol 2014;25(1):18–32.
[5] Bastos AP, Onuchic LF. Molecular and cellular pathogenesis of autosomal dominant polycystic kidney disease. Braz J Med Biol Res 2011;44(7):606–17.
[6] Ravichandran K, Edelstein CL. Polycystic kidney disease: a case of suppressed autophagy? Semin Nephrol 2014;34(1):27–33.
[7] Stanley RE, Ragusa MJ, Hurley JH. The beginning of the end: how scaffolds nucleate autophagosome biogenesis. Trends Cell Biol 2014;24(1):73–81.
[8] Levine B, Kroemer G. Autophagy in the pathogenesis of disease. Cell 2008;132(1):27–42.

[9] Glick D, Barth S, Macleod KF. Autophagy: cellular and molecular mechanisms. J Pathol 2010;221(1):3–12.
[10] Zhu P, Sieben CJ, Xu X, Harris PC, Lin X. Autophagy activators suppress cystogenesis in an autosomal dominant polycystic kidney disease model. Hum Mol Genet 2017;26(1):158–72.
[11] Petkov PM, Cassell MA, Sargent EE, Donnelly CJ, Robinson P, Crew V, et al. Development of a SNP genotyping panel for genetic monitoring of the laboratory mouse. Genomics 2004;83(5):902–11.
[12] Gouttenoire J, Valcourt U, Bougault C, Aubert-Foucher E, Arnaud E, Giraud L, et al. Knockdown of the intraflagellar transport protein IFT46 stimulates selective gene expression in mouse chondrocytes and affects early development in zebrafish. J Biol Chem 2007;282(42):30960–73.
[13] Subramanian A, Tamayo P, Mootha VK, Mukherjee S, Ebert BL, Gillette MA, et al. Gene set enrichment analysis: a knowledge-based approach for interpreting genome-wide expression profiles. Proc Natl Acad Sci U S A 2005;102(43):15545–50.
[14] Song X, Di Giovanni V, He N, Wang K, Ingram A, Rosenblum ND, et al. Systems biology of autosomal dominant polycystic kidney disease (ADPKD): computational identification of gene expression pathways and integrated regulatory networks. Hum Mol Genet 2009;18(13):2328–43.
[15] Woo YM, Bae JB, Oh YH, Lee YG, Lee MJ, Park EY, et al. Genome-wide methylation profiling of ADPKD identified epigenetically regulated genes associated with renal cyst development. Hum Genet 2014;133(3):281–97.
[16] Yu J, Carroll TJ, McMahon AP. Sonic hedgehog regulates proliferation and differentiation of mesenchymal cells in the mouse metanephric kidney. Development 2002;129(22):5301–12.
[17] Zhou JX, Li X. Apoptosis in polycystic kidney disease: from pathogenesis to treatment editor. In: Li X, editor. Brisbane (AU), 2015, editor. Polycystic kidney disease; 2015. Brisbane (AU).
[18] Hanaoka K, Guggino WB. cAMP regulates cell proliferation and cyst formation in autosomal polycystic kidney disease cells. J Am Soc Nephrol 2000;11(7):1179–87.
[19] Ecder T, Melnikov VY, Stanley M, Korular D, Lucia MS, Schrier RW, et al. Caspases, Bcl-2 proteins and apoptosis in autosomal-dominant polycystic kidney disease. Kidney Int 2002;61(4):1220–30.
[20] Lee MS, Hwang KS, Oh HW, Ji-Ae K, Kim HT, Cho HS, et al. IFT46 plays an essential role in cilia development. Dev Biol 2015;400(2):248–57.
[21] Martinez-Lopez N, Athonvarangkul D, Mishall P, Sahu S, Singh R. Autophagy proteins regulate ERK phosphorylation. Nat Commun 2013;4:2799.
[22] Avalos Y, Pena-Oyarzun D, Budini M, Morselli E, Criollo A. New roles of the primary cilium in autophagy. Biomed Res Int 2017;2017:4367019.
[23] Ravichandran K, Zafar I, Ozkok A, Edelstein CL. An mTOR kinase inhibitor slows disease progression in a rat model of polycystic kidney disease. Nephrol Dial Transplant 2015;30(1):45–53.
[24] Zafar I, Ravichandran K, Belibi FA, Doctor RB, Edelstein CL. Sirolimus attenuates disease progression in an orthologous mouse model of human autosomal dominant polycystic kidney disease. Kidney Int 2010;78(8):754–61.
[25] Warner G, Hein KZ, Nin V, Edwards M, Chini CC, Hopp K, et al. Food restriction ameliorates the development of polycystic kidney disease. J Am Soc Nephrol 2016;27(5):1437–47.
[26] Tao Y, Kim J, Schrier RW, Edelstein CL. Rapamycin markedly slows disease progression in a rat model of polycystic kidney disease. J Am Soc Nephrol 2005;16(1):46–51.
[27] Wahl PR, Serra AL, Le Hir M, Molle KD, Hall MN, Wuthrich RP. Inhibition of mTOR with sirolimus slows disease progression in Han:SPRD rats with autosomal dominant polycystic kidney disease (ADPKD). Nephrol Dial Transplant 2006;21(3):598–604.
[28] Wu M, Wahl PR, Le Hir M, Wackerle-Men Y, Wuthrich RP, Serra AL. Everolimus retards cyst growth and preserves kidney function in a rodent model for polycystic kidney disease. Kidney Blood Press Res 2007;30(4):253–9.
[29] Walz G, Budde K, Mannaa M, Nurnberger J, Wanner C, Sommerer C, et al. Everolimus in patients with autosomal dominant polycystic kidney disease. N Engl J Med 2010;363(9):830–40.
[30] Serra AL, Poster D, Kistler AD, Krauer F, Raina S, Young J, et al. Sirolimus and kidney growth in autosomal dominant polycystic kidney disease. N Engl J Med 2010;363(9):820–9.
[31] Shillingford JM, Leamon CP, Vlahov IR, Weimbs T. Folate-conjugated rapamycin slows progression of polycystic kidney disease. J Am Soc Nephrol 2012;23(10):1674–81.